2025 NDIA MICHIGAN CHAPTER
GROUND VEHICLE SYSTEMS ENGINEERING
AND TECHNOLOGY SYMPOSIUM
AUTONOMY, ARTIFICIAL INTELLIGENCE, & ROBOTICS (AAIR) TECHNICAL SESSION
AUG. 12-14, 2025 - NOVI, MICHIGAN

COMMUNICATION NETWORK CONSTRUCTION BEHAVIORS FOR ROBOTIC CONVOYING

Charles Noren*[1], Sahil Chaudhary*[1], Burhanuddin Shirose[1], Bhaskar Vundurthy, PhD[1], and Matthew Travers, PhD[1]

[1]Carnegie Mellon University, Pittsburgh, PA

ABSTRACT

We develop a set of communications-aware behaviors that enable formations of robotic agents to travel through communications-deprived environments while remaining in contact with a central base station. These behaviors enable the agents to operate in environments common in dismounted and search and rescue operations. By operating as a mobile ad-hoc network (MANET), robotic agents can respond to environmental changes and react to the loss of any agent. We demonstrate in simulation and on custom robotic hardware a methodology that constructs a communications network by "peeling-off" individual agents from a formation to act as communication relays. We then present a behavior that reconfigures the team's network topology to reach different locations within an environment while maintaining communications. Finally, we introduce a recovery behavior that enables agents to reestablish communications if a link in the network is lost. Our hardware trials demonstrate the systems capability to operate in real-world environments.

Citation: C. Noren, S. Chaudhary, B. Shirose, B. Vundurthy, M. Travers, "Communication Network Construction Behaviors for Robotic Convoying," In *Proceedings of the 2025 Ground Vehicle Systems Engineering and Technology Symposium (GVSETS)*, NDIA, Novi, MI, Aug. 12-14, 2025.

1. INTRODUCTION

Robotic teams have repeatedly demonstrated the capability to effectively search dangerous or difficult-to-reach areas. Such results were most prominently demonstrated during the Defense Advanced Research Projects Agency (DARPA) Subterranean (SubT) Challenge [1]. Given that many of the DARPA SubT test environments were not equipped with communications infrastructure, performer teams often simultaneously completed search and rescue tasks while building a mobile wireless ad-hoc network (MANET). The constructed MANET was often dependent on "drop nodes" –communication relays that were physically "dropped" from robotic platforms– as they explored the environment. In many applications, including dismounted operations, the need for communications between robotic

* indicates equal contributions

agents is still present, but relying purely on drop-node-based strategies has many undesirable features. Such approaches can be time-consuming for human operators, as they may need to clean-up or collect the drop nodes, and the network topology can be difficult to modify once the nodes are deployed. In this work, we build on our SubT experience by truly observing the "*mobile*" name of a MANET. We introduce and integrate a series of MANET construction and modification behaviors for teams of robotic agents that travel in a convoy formation. Our aim is to begin a discussion on how to develop automated communications-aware robotic systems that can operate in communications-deprived environments without relying on human operators (e.g., the warfighter, disaster response team members, etc.). We argue that operating as a MANET is a core underlying technology to multi-agent operations and then demonstrate the application of such technologies to multi-robotic-agent formation movement problems in cluttered environments.

We consider missions where the robotic agents are required to move throughout an environment while remaining in constant contact with a central base station. Both the base station and the robotic agents are equipped with wireless communication capabilities (nodes) that allow the base station and the agents to communicate with each other at distance under nominal conditions. Agents move through the environment as part of a formation, normally a convoy, to provide mutual support to each other during the traversal. As agents move through the environment, the quality of the inter-agent communications is affected by objects in the environment and the distance between the agents. We require that connections between the base station and a multi-agent formation are required to maintain a measure of communications strength in order to ensure constant communication between the agents and the base station.

To achieve this operating concept, we introduce a MANET topology construction technique for robotic systems with mobile communication nodes. We introduce three behaviors: 1) the MANET construction technique for formations, 2) a formation control algorithm that maintains the network structure while the vehicles move through the environment, and 3) a set of individual agent behaviors to reconnect the network topology if a node in the network fails. We demonstrate these algorithms in simulation and on robotic hardware for a small team of robotic agents.

The remainder of this manuscript is structured as follows. We begin with an overview of the relevant literature, much of which is concerned with the DARPA Subterranean Challenge and techniques and technologies derived from it. Following this, we introduce our construction behavior and describe two "recovery behaviors": algorithms that 1) optimize the placement of communication nodes and 2) repair the communications network in the face of node failure or loss of communications. We demonstrate these algorithms in both simulation and robotic hardware and conclude the paper with some additional commentary and future directions.

2. RELATED WORK

As noted in the previous section, this work is the latest in a series of works derived from the DARPA Subterranean Challenge [1]. As the "Systems" SubT performer teams were required to complete a challenge with similar requirements to our work (i.e., operating in communications-deprived environments), we first provide a brief overview of the different systems developed by each of the SubT performer teams before surveying other relevant communications-aware multi-agent systems literature.

In particular, we would like to highlight Team CERBERUS [2], Team CoSTAR [3,4], Team NCTU [5], and Team Explorer [6]. For multi-agent operations, many of the robotic systems deployed in the different teams required inter-agent communication. Many of the communication solutions used in these approaches resulted in teams constructing a "communication backbone" that would allow information sharing (e.g., environmental maps, odometry information, detected objects, etc.) with the other agents in the team [7]. Each of the aforementioned teams relied on both robotic agents and a set of "dropped" communication nodes to ensure that the agents in the system would remain in communication with the base station. Certain teams, such as Team CERBERUS, relied on a "Human Supervisor" to drop additional communication nodes given the challenges with ascertaining consistent measures of communications performance in SubT environments [2]. Team CoSTAR designed a robotic behavior that considered both environmental factors, relative line-of-sight and coverage, and network conditions to determine if a drop should occur [4]. Team NCTU's solution evolved over the DARPA SubT challenge, with early drop nodes being augmented and replaced with mobile nodes mounted to small wheeled robotic platforms which could be moved in response to poor-communications environments [5]. Team Explorer designed both a set of distance-based heuristics for both line-of-sight (LOS) and non-line-of-sight (NLOS) operations alongside a map prediction algorithm to determine where to drop nodes [6, 8]. Our proposed system takes components learned from each of the SubT performer teams: human supervision (CERBERUS), network-conditioned-based drops (CoSTAR), mobile communications nodes (NCTU), and NLOS (Explorer) operations.

Clearly, the design of network construction algorithms is highly dependent on the placement of communication relays throughout the environment. This placement is influenced not only by the environment itself, but also by the current known information about the environment and the communications system. While both our operating conditions and the environments the SubT agents performed in were *a priori* unknown, *a priori* known environments give rise to computational geometry techniques for sensor placement strategies in wireless sensor networks [9]. Certain techniques frame the problem as a variant of the Art Gallery Problem, a visibility-based approach to predicting sensor placement. Solutions to the Art Gallery Problem minimize the number of sensors (guards) required to cover a (classically) polygonal area [10]. Different sensor models modify the expected visibility of the guards, yielding different solutions to these optimization problems. Common modifications include limiting the visible range of any placed guard [10], distance-based visibility fading [11], and visibility through a limited number of walls (k-transmitters problem) [12]. While some of these geometric approaches translate to robotic systems, the quality of the information traveling across the communications system also comes into play.

The variety of different measures of communications quality in wireless transmission is reflected even with the variety of communications metrics considered by the different performer teams in the DARPA SubT Challenge. Certain teams (CERBERUS) side-stepped this issue entirely, noting that common radio signal strength indicators (RSSI) were often not reliable in subterranean environments citing previous work in underground environments: [13, 14]. Yet in certain Subterranean environments, other teams (NCTU and Explorer) relied on RSSI to conduct node drops [5, 6]. Finally, utilizing signal-to-noise (SNR) has been considered in multiple works adjacent to Team CoSTAR [3] with a focus on planetary exploration. Predicting these communications metrics is challenging, and recent work has leveraged machine learning techniques to predict a 5G signal strengths in an indoor environments [15]. Such techniques can be useful if direct access to SNR values is unavailable or if the environmental SNR values need to be predicted beforehand.

The relay placement problem is also highly related to communications-aware motion planning and operations. These works often consider a single aspect of inter-agent communications to address. A communications-denied environment is more challenging, as elements of the environment (e.g., adversarial agents) may block intra-team communications. Wang, et al. [16] developed a jamming-resilient path planning algorithm for Unmanned Aerial Vehicles (UAVs) based on Deep Reinforcement Learning. The approach learns the signal-to-interference-plus-noise ratio mapping for the environment while taking into consideration the effects of a dynamic jammer. Aside from the aforementioned SubT works, maintaining communications during environmental exploration in communications-deprived environments is also well-studied. Woosley, et al. [17] considered the problem of simultaneous exploration and information collection in an unknown environment. Locations for exploration and information collection were selected using a Gaussian Process that modeled information entropy and communications signal strength. However, the considered agents did not operate in formations and were not required to maintain communication with an operator interface, which differentiate our considered problem space. Another approach involves exploring unknown environments while intermittently sharing maps at scheduled rendezvous locations, without having to use a relay network to continuously maintain connectivity with a base station [18]. This method works well to quickly map out and explore an unknown area. However, it assumes that connectivity to the base station can be broken intermittently which is not allowable in our operations.

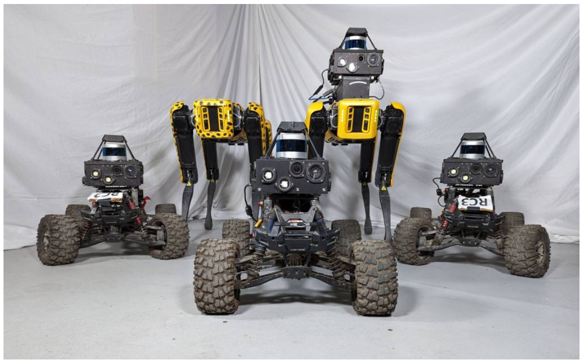

Figure 1: The team of robotic agents utilized in this work. The quadruped agents are compatible with the presented approaches, but are not demonstrated herein.

3. TECHNICAL APPROACH

In order to ensure communications during a robotic mission, we propose a graph-based mobile ad-hoc network (MANET) construction system inspired by our experience in the DARPA Subterranean Challenge. We build on these experiences by replacing dropped "communication nodes" with a formation of cooperative ground agents. We first provide an overview of the hardware systems that constitute our approach and then discuss the proposed behaviors.

3.1. System Overview

The developed robotic system consists of a heterogeneous team of robotic platforms

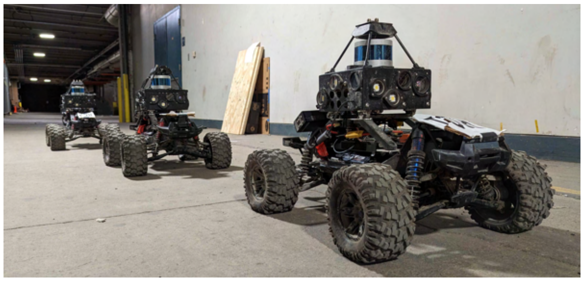

Figure 2: A multi-agent convoy consisting of three vehicles. Heterogeneous convoys are also possible using our system.

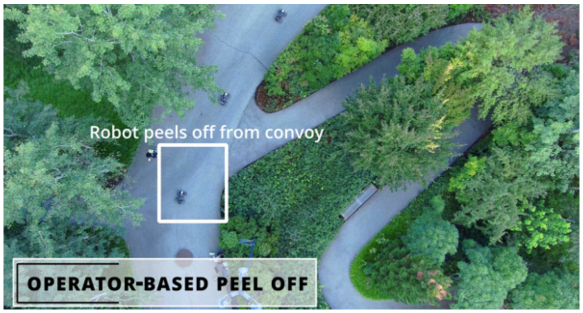

Figure 3: An operator commanded "peel-off" in an urban environment.

paired alongside an operator interface (i.e., a basestation), that is also referred to as "BST" in the rest of this manuscript. As shown in Figure 1 agent team may consist of either legged or wheeled platforms. Each platform is equipped with a custom-built payload containing on-board compute, sensing (Light Detection and Ranging (LiDAR), Inertial Measurement Unit (IMUs), and Cameras), and communications radios. This payload allows the agents to simultanesouly map their environment and compute their odometry relative to the position of the operator interface. The system uses Robot Operating System (ROS) and the Data Distribution Service (DDS) middleware for communication between the base station and robotic agents. For a comprehensive discussion of the system architecture, see [19].

Of particular note is the system operating concept. In order to decrease operator workload and improve system redundancy, the system has been designed to perform multi-agent platooning (convoying) in a linear formation [20]. This platooning behavior requires multiple agents to form a linear formation and travel together toward a common mission objective. The formation order is determined autonomously or by a human operator. The agents can then travel autonomously to the mission objective or in a guided manner, where an operator only controls the lead robot. An example of a wheeled platoon is shown in Figure 2.

While autonomous platoon formation and travel has been handled in prior works from our group, we desire a methodology to ensure that the platoon of agents remains in communication with the base station during the entire operation. Initially, we relied on an operator to manually "peel-off" an agent from the convoy when the convoy was about to leave communication range. Triggering a peel-off would cause the last agent in the convoy to leave the convoy and stop. When the agent stopped, it effectively acted as a **communication node**, extending the effective communications boundary. An example of such a peel-off is shown in Figure 3. We thus define an automated **peel-off behavior** as a maneuver executed by an agent participating in a convoy that causes the agent to 1) leave the formation, 2) come to a complete stop, and 3) relay communications to other assets in the system. We modified this manual peel-off to be callable by the lead agent of an autonomous convoy. This enables the lead agent to direct the follower agents to act as communication nodes if a set criterion is met. We describe this behavior as an "automated peel-off" behavior. We describe the criterion for peel-off in the following section (Section 3.2).

3.2. Network Construction Behavior

Determining when to "peel-off" agents in an automated manner is fundamentally connected to the connectivity and interactions between system assets. Graph data structures provide a convenient means to represent this interrelatedness of assets in our system. In our communications systems, this interrelatedness of assets exists in at least two representative aspects. There is an inherent coupling between 1) the physical (spatial) representation and 2) the signal strength layer of a communications network. For MANETs, the mobile nature of a robotic system makes this coupling even more prevalent. We pose our network construction behavior as a graph analysis problem where the network topology changes as the robotic agents navigate through the environment.

The network topology is constructed from a set of n communications-enabled assets, including: 1) operator interfaces (e.g., base station), 2) pre-placed environmental communications infrastructure (if any), 3) individual robotic agents, and 4) formations/teams of robotic agents. For simplicity, we enumerate the total list of assets $\mathcal{C} = \{c_0, c_1, c_2, \ldots, c_{n-1}, c_n\}$ with index set $\mathcal{I} = \{0, 1, 2, \ldots, n-1, n\}$. We define the set of agents in the asset list $\mathcal{A} \subset \mathcal{I}$ with corresponding index set $\mathcal{I}_a \subset \mathcal{I}$, and, for simplicity, denote asset c_0 as the operator interface (e.g., base station). As these assets represent physical entities (e.g., a robotic agent), we define a mapping that takes an asset index and returns its physical location with respect to a predetermined common reference frame (e.g., the base station). We define $p : \mathcal{C} \to \mathbb{R}^n$ to represent this function.

We represent the relationships between the assets using a pair of undirected weighted graphs. The first graph, $G_d = (V, E_d, w_d)$, captures the inter-asset distances, i.e., the relative spatial positions, between the assets. In this graph, each vertex $v_i \in V \subseteq \mathcal{C}, i \in \mathcal{I}$ represents an asset, and the edges connecting all vertices are assigned a weight equivalent to the ℓ_2-distance between agents (i.e., $w_d = d(v_i, v_j) = \ell_2(p(v_i), p(v_j)), v_{i,j} \in V$). Note that while we overload the notation of $p(\cdot)$, its meaning remains the same. Each asset may also be represented via the network logical layer topology, or the communications connections and relative signal strength the asset has to other assets. We define this representation as a "**communications graph**", and denote it: $G_c = (V, E_c, w_c)$. In this definition, the vertex set definition remains consistent with G_d (i.e., the vertices represent assets), but the edge set definition does not. Edges now represent available communications between assets, and are weighted by a corresponding weighting function, $w_c = \text{COMM}(v_i, v_j,), v_{i,j} \in V$. As discussed in Section 2, this $\text{COMM}(\cdot)$ function can represent a number of different indicators for signal strength. Finally, note that both graphs are dynamic in-so-much that the relationships between the agents may change during operation (e.g., agent motion through the environment).

While the communications graph captures the relative communications strengths between assets, it does not inherently indicate *when* an agent should be "peeled-off" from a convoy. We propose that the establishment of a communication node (i.e., a "peel-off") should occur in response to a potential loss of communication between the agents and the base station. We model the proposed mechanism as a restriction that for every agent in the agent list $\mathcal{I}_A$, there must exist at least one path in a communications graph that starts at the base station v_0, and ends at an agent, v_i where all edge weights maintain a value greater than a minimum allowable edge weight. If we define this minimum allowable edge weight as C_{THRESH} and a path in the communications graph as a set of edges between two different vertices ($\pi(v_i, v_j)$, $v_i \in V, v_j \in V, v_i \neq v_j$), then we seek to ensure that $w_c(e) \geq \text{C}_{\text{THRESH}} \, \forall \, e \in \pi(v_0, v_i)$, $\forall \, i \in \mathcal{I}_A$. For notational simplicity, we drop the dependence on v_0 and choose to represent paths between the operator interface and an agent i via a single argument (i.e., $\pi(v_0, v_i) = \pi(v_i)$).

To ensure this restriction is observed, we construct a maximin spanning tree, $T \subseteq G_c$, on the communications graph rooted at the operator interface (v_0). The tree is constructed such that the edge weights associated with edges included in tree T maximize the strongest "weakest" link between a parent node and its child node in the tree. Concretely: for each non-root vertex, v_i, connected by edge (v_i, v_j) to its parent node, v_j, an associated edge weight CMET$(v_i, v_j) \in \mathbb{R}^+$ is chosen such that CMET(v_i, v_j) represents the strongest "weakest" link for v_i in the communications graph. As the spanning tree T spans all vertices included in communications graph, and by ensuring that CMET$(v_0, v_i) \geq$ C$_{\text{THRESH}}$, $v_i \in V \in T$, we ensure that at least one path between v_0 and v_i exists such that the minimum edge weight is observed for all edges in the tree.

We describe any communication nodes that represent the operator interface or an agent that has performed a peel-off behavior as a **central node**. For ease of reference, we collate these central nodes into a set: CN. Note that, initially, $CN \leftarrow \{v_0\}$ as the list of central nodes always includes the node representing the operator interface. Thus, these central nodes represent our version of the vital "communications backbone" described by many DARPA SubT works [7]. Maintaining a connection to at least one central node guarantees a communication pathway to the operator interface.

Thus, we can define the network topology $\mathcal{N}$ of the system by considering elements of the communications graph. The network topology itself consists of a "communications backbone" of central nodes and the remaining mobile agents. There exists an effective communications boundary $\mathcal{B}(\mathcal{N})$ created by all the assets in the system. The strength of the system's communications within this limit as observed by the system assets is no less than C$_{\text{THRESH}}$. That is, $\mathcal{B}$ forms a level set $L = \{x \in \mathbb{R}^n \mid \mathcal{B}(x) =$ C$_{\text{THRESH}}\}$, where $x \in \mathbb{R}^n$ denotes a spatial location in the environment. This communications boundary delineates the limit of the MANET coverage area, crossing which will lead to loss of communication for that agent. The automated peel-off behavior described previously enables agents to, in a methodological way, extend the communications boundary $\mathcal{B}$ by tasking an agent to at as a communication node. This communication node extends the current communications boundary, thus guaranteeing that the remaining agent remain in contact with the operator interface with a minimum communications strength C$_{\text{THRESH}}$.

3.3. Re-optimization Behavior

As the robotic formation travels through the environment, we observe that the peeled robotic agents form a type of kinematic "chain" from the base station to the target. By analogy to a planar robotic manipulator, the agents would be synonymous to joints, and inter-agent distances synonymous to robotic links. Please, see Fig. 4 for a toy example depicting our observation. In effect, the central nodes form a stationary network topology configuration for a particular mission objective. However, if the mission objective is changed or an additional objective is provided, the central node configuration may not be adequate to provide communications coverage to that new objective. For small deviations from the initial configuration, we suggest that modeling the agent convoy as a pseudo-robotic manipulator. Using this methodology, we can locally re-optimize the position of each robotic agent through

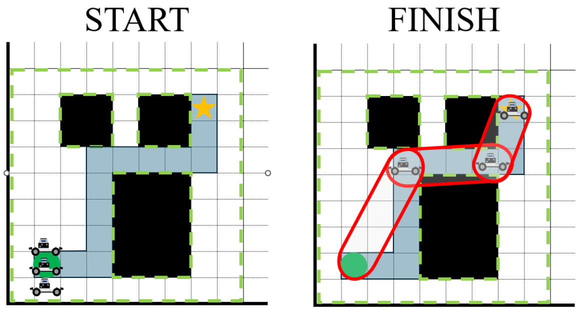

Figure 4: A toy example provided by a pair of diagrams with the starting configuration on the left and the ending configuration on the right. In the diagrams, a team of three robotic agents starts at a base station location (green circle) and are tasked with traveling to an objective (gold star) while avoiding the objects (black). The agents travel as a convoy through the dark blue squares, peeling-off at different intervals. In the final configuration, the agents are positioned similar to a kinematic chain (outlined in red).

inverse kinematic techniques and extend the communications boundary to achieve the next mission objective.

Consider N agents participating in a convoy whose locations must be optimized in response to a new objective with $x_g \in \mathbb{R}^n$. The current spatial location of each agent is given by $x_i \in \mathbb{R}^n$ with $i \in \{1, 2 \ldots, N-1, N\} = \mathcal{I}_C$. Furthermore, require the order of $\mathcal{I}_C$ to represent adjacent agents in the chain (i.e., agents connected by the same "link", this can be found using the maximin tree). For convenience, we also define set $\mathcal{I}_{C \setminus N} = \{0, 1, \ldots, N-2, N-1\}$, with 0 (and the corresponding x_0) representing the base station position. In order to optimize the set of agent positions, we concatenate the decision variables into a vector: $X \in \mathbb{R}^{(n \cdot N) \times 1}$. For convenience, we create a similar vector for the goal state, X_g by concatenating the goal state N times. We overload function $d(x_i, x_j) : \mathbb{R}^n \times \mathbb{R}^n \rightarrow \mathbb{R}$ which measures the Euclidean distance between two points x_i and x_j.

For this behavior, we consider a communications model with distance fading but no obstacle attenuation, where the maximum allowable distance between two agents such that they remain in communication is given as r_C. On sequential agents i and j, we can then form a quadratic constraint of the form

$$\text{CB}(i, j) = d(x_i, x_j) - r_C^2 \leq 0, \tag{1}$$

which captures the allowable spacing between agents to ensure the communications boundary. While this work only considers simple geometric constraints consistent with our communications system model, we recommend that this constraint be modified in future studies to a more complex model.

In this re-optimization method, while the communication links are not influenced by the presence of obstacles, the agents themselves cannot achieve a position inside an obstacle. As the agents map the environment, they each contribute to a global occupancy grid consisting of constant square cells, $\mathcal{G}$, which delineates the space into object-free and object-occupied space. By iterating through the set of unoccupied cells in the occupancy grid, $\mathcal{G}_U$, we can enforce a constraint on the agents' positions. We do so by convexifying each occupied cell, $u \in \mathcal{G}_U$, by a capsule of constant radius r_o, where $r_o > \sqrt{\frac{l^2}{2}}$ and l represents the resolution of a occupancy grid cell. If we represent the center of a grid cell as x_u, then we can write the object avoidance constraints on the between agent i and occupied cell u as

$$\text{OB}(i, u) = r_o^2 - d(x_i, x_u) \leq 0. \tag{2}$$

Combining the above constraints yields a quadratically constrained quadratic program that can be solved on the base station to re-optimize the location of the agents. This program takes the form:

$$\min_{X} \quad \frac{1}{2}(X - X_G)^T (X - X_G) \qquad (3)$$

$$\text{subject to} \quad \text{CB}(i,j),\ i \in \mathcal{I}_{C\setminus N},\ j = i+1, \qquad (4)$$

$$\text{OB}(i,u), i \in \mathcal{I}_c, u \in \mathcal{G}_U \qquad (5)$$

Note that we further post-process the results to ensure that no path experiences large deviations from the original vehicle configurations. To bias the results away from large deviations, we perform a local change of coordinates for X, biasing the vector towards the initial positions of the agents: $X' = X - X_{IC}$ with X_{IC} representing the initial configuration of the vehicles.

3.4. Network Repair Behavior

During real-world operations, robotic systems are prone to failure (e.g., agent onboard power loss). If such a failure afflicted a single (or multiple) central node during operation, the communications network topology may become separated into at least two disconnected subgraphs or cause the an edge in the communications graph to obtain an insufficient edge value below C_{THRESH}. In order to improve system robustness in response to such failures, we propose a communications network repair behavior that reallocates available agents to replace failed central nodes in order to re-establish communications with the root node of the maximin communications tree.

The proposed communications network repair behavior is described in Algorithm 2. The goal of the behavior is to drive agents back towards the communications boundary of the new communications network topology that excludes the failed node. The algorithm runs locally on each agent (node v_a) and is activated when the signal strength between the agent and the agent's parent node (node v_p) in the maximin communications tree falls below the threshold value (i.e., $\text{CMET}(v_a, v_p) < \text{C}_{\text{THRESH}}$). Note that this implies that central nodes may also move to repair the network if their signal strength falls below C_{THRESH}. Given that Algorithm 2 runs on each agent, the motion of an agent acting as a central node could activate the recovery behaviors of any agents dependent on v_a.

Before providing an overview of the algorithm, we outline the underlying assumptions of our approach. We first assume that the root node of the maximin communications tree (i.e., the central base station) does not fail and that all nodes have the same communications capabilities. To enable an agent to return to the communications boundary of its parental central node, the agent stores the locations of all central nodes in the network onboard. Define the set of central node locations as $CN_L = \{x_0^{cn}, ..., x_n^{cn}\}$, where $x_i^{cn} \in \mathbb{R}^n$ represents the location of central node i (e.g., $x_i^{cn} \in \mathbb{R}^2$ for a planar environment) and x_0 represents the position of the root node. In the case of central node failure, these locations represent the most likely locations to be able to re-establish the network. Finally, we assume that all locations in CN_L are reachable by all robotic agents from any location in the environment.

For convenience, we define a subroutine (Algorithm 1) to find the closest central node to robotic agent a. Define the position of agent a as $x_a \in \mathbb{R}^n$ and the visited set of central nodes as $\mathbb{V} \subset CN_L$. We first find the index of the central node closest (based on Euclidean distance) to a position x, (e.g., agent x_a) that is yet to be visited (Line 1), and then return that node's location (Line 2).

Given these assumptions and Algorithm 1, we propose the Network Repair Behavior in Algorithm 2. We first target the parent node of the agent in the maximin communications tree (Line 2) as it is assumed that the parent

Algorithm 1 Closest Central Node (CCN)

```
Require: $CN_L, \mathbb{V}, x$
Ensure: $x_{cn} \in CN_L$    ▷ Closest central node
1: $i = \arg\min(d(x, x_i)\, \forall\, i \in CN_L, i \notin \mathbb{V})$
2: return $x_{cn} = CN_L[i]$    ▷ get $i$ from $CN_L$
```

is the closest node, and move along a path to the parent node (which is guaranteed to exist via our earlier assumptions) in Line 3. We first check to see if we are "close enough" (less than a threshold, d_{min}) to the target node's location, x_g, on Line 3, and continue moving towards x_g if we are not (Line 9). If the distance between the target node x_g (initially, x_p, (Line 1)) and agent a becomes less than d_{min} and CMET$(v_a, v_p) <$ C

Algorithm 2 Network Repair Behavior

```
Require: $x_a, x_p, CN_L, t$, COMM$(v_a, v_p)$
1: Initialize $\mathbb{V} \leftarrow \emptyset$, $x_g = x_p$
2: while COMM$(v_a, v_p) <$ C$_{\text{THRESH}}$ do
3:     if $d(x_a, x_g) < d_{min}$ then
4:         if $d(x_a, x_0) < d_{min}$ then
5:             break    ▷ reached root node
6:         $\mathbb{V} \leftarrow \mathbb{V} \cup \{v_p\}$
7:         $x_g \leftarrow$ CCN$(CN_L, \mathbb{V}, x_a)$
8:         $v_p = CN[g]$    ▷ update $v_p$ to $v_t$
9:     Move towards $x_g$    ▷ for $t$ seconds
```

An important point to note is that the algorithm is guaranteed to recover communications as long as a path exists to the root node of the maximin tree, causing the agent to ultimately reach the central base station (root node) location, x_0, if it could not regain communications elsewhere.

4. NUMERICAL SIMULATIONS

The proposed communications network construction techniques and recovery behaviors were implemented in simulation. The numerical simulations are performed in environments that are representative of different real-world scenarios, including buildings, cities, and natural environments. Unless noted otherwise, none of the test environments include existing communications infrastructure that the robotic team could utilize during its movement through the environment.

We first demonstrate our network construction capabilities on a set of maps from a Multi-Agent Pathfinding (MAPF) benchmark [21]. These results demonstrate the evolution of the network topology in complex environments using a communications model to guide the placement of communication nodes. We also demonstrate both recovery behaviors in simulation. The network repair simulation environments are modeled in Gazebo. These studies reflect how communication node failure is addressed using Algorithm 2.

4.1. Network Construction Studies

We first simulate a series of missions that require a team of robotic agents to travel through different environments with no existing communications infrastructure. The objective of this set of tests is to determine the required number of robotic agents needed to construct a communications network between an initial start location and a goal location. The environments are drawn from Stern's Multi-Agent Pathfinding benchmark [21]. Each environment is represented as an occupancy map, where the measure of occupancy denotes whether a robotic agent may traverse a cell in the occupancy map. Although the network construction algorithms described in Section 3 are not dependent on an *a priori* possession of each environment's occupancy map, each map is assumed to be known beforehand in order to compute the shortest path between the start and goal states (e.g., via Dijkstra's Algorithm). Given this shortest path between the start and goal states, a communications model is then propagated from an agent (or the base station) at the initial start state along the path. Every robot that is deployed as a communication node then acts as a further source of this communication model, enlarging the communication-accessible area for the other robotic agents.

Although robotic agents are incapable of traversing through occupied cells, in these studies, we assume that the communications model is capable of such obstacle penetration. We represent our communications system using a communication model with distance fading: wherein the communications signal strength is inversely proportional between the source and receiver. This model is further augmented with additional signal attenuation arising from occupied cells. This additional signal attenuation is assumed at a rate of 20 [cell^{-1}] (e.g., a 20 [unit] reduction in signal strength every 1 [cell] encountered).

We provide an overview of the results of our simulations in Figure 5. We also include a number of reference images to three maps, including: 1) *lak303d*, 2) *Boston_0_256*, and 3) *Berlin_1_256*, to depict the constructed network topologies. For each map, we generate one-hundred different start-goal configurations on the same occupancy map.

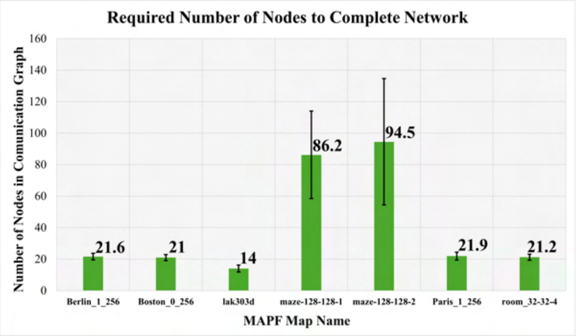

Figure 5: A summary of the network construction tests demonstrating the required number of nodes needed to construct a communications network in the MAPF environments.

Each starting position is denoted with a green circle and each ending position is denoted with a red circle. Using the communication model above, communication nodes are deployed whenever the signal strength falls below the threshold of 10 (i.e., $C_{\text{Thresh}} = 10$). Each communication node that is deployed is represented by a gold circle. The path along which the team travels is shown in orange.

Each environment demonstrates a varying amount of object clutter that must be navigated by the robotic agents. Large numbers of deployed nodes appear to arise in environments with sharp corners and on objects that must be traversed around that continuously block line-of-sight (*Berlin_1_256*, Fig. 7). We also see that tight corridors, such as near the goal location in Fig. 6, generally require large numbers of communication nodes to ensure communication quality along the passage.

Remark (Re-optimization)**.** *We additionally include a re-optimization of the nodal positions considered in Figure 7 to a new configuration in Figure 9. The configuration change is motivated by the new goal location that the agents are required to visit. The contract of the kinematic chain reflects a difference in required number of nodes (29 to 26), but the remaining agents largely remain in place.*

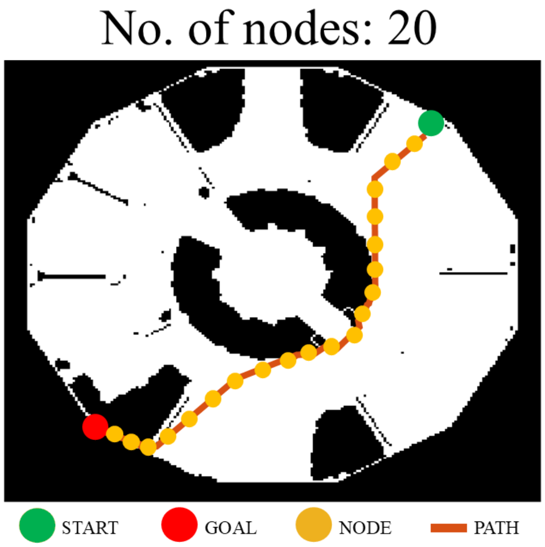

Figure 6: *lak303d* Environment Construction

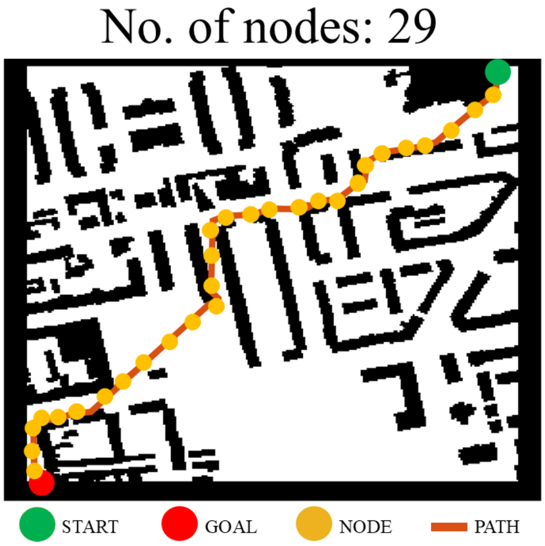

Figure 7: *Berlin_1_256* Environment Construction

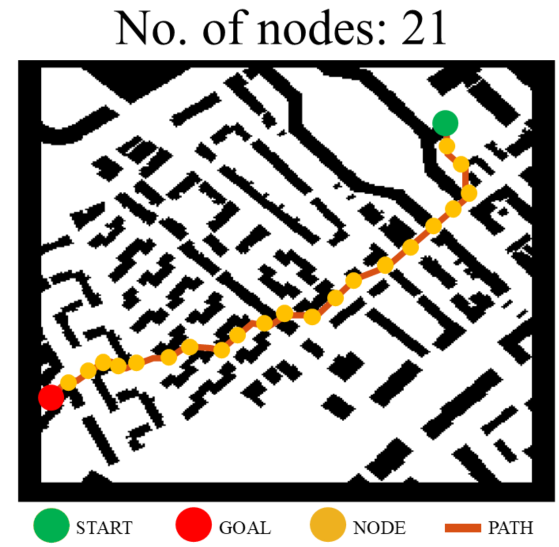

Figure 8: *Boston_0_256* Environment Construction

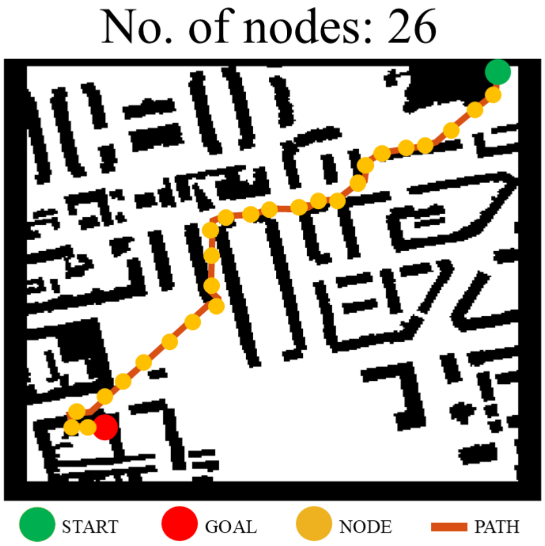

Figure 9: *Berlin_1_256* Environment Re-optimization

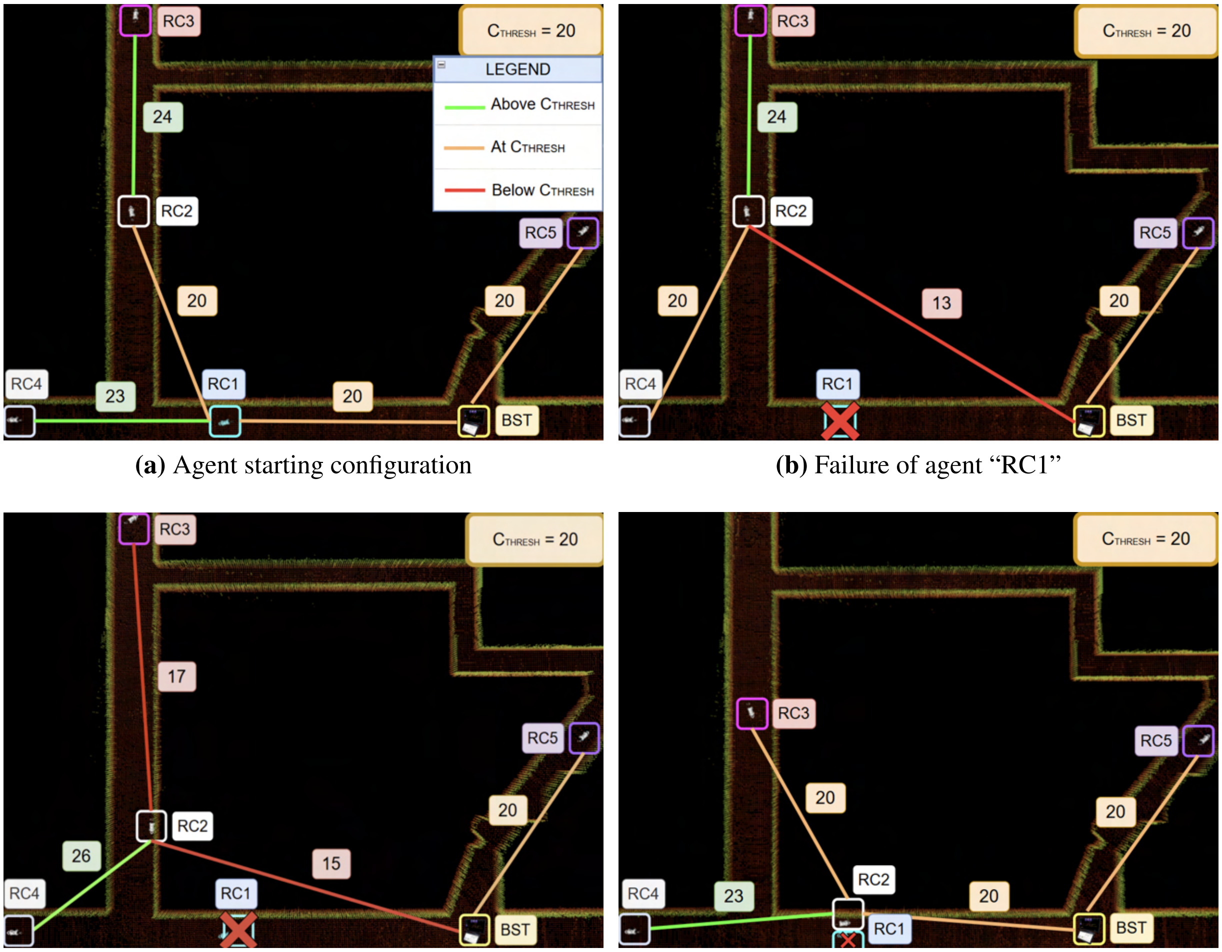

(a) Agent starting configuration

(b) Failure of agent "RC1"

(c) Agent "RC2" moves to repair the network

(d) Agent "RC3" goes below $\mathrm{C_{THRESH}}$ & repairs network

Figure 10: The first simulation study demonstrates the network repair behavior described in Algorithm 2. The study demonstrates the cascading effect of the network repairing process on multiple agents ("RC2" and "RC3").

4.2. Network Repair Studies

This section demonstrates the efficacy of Algorithm 2 in different simulation environments. As in the previous simulation section, we adopt a scaled inverse model for our communications system. The communication metric, $\mathrm{COMM}(\cdot)$, was defined to be inversely proportional to distance and scaled by a scaling factor k. This scaling factor is a tunable parameter to change the effective range of the communications model, with a larger scaling factor correlated to a larger communications boundary. For example, for an agent 10 [m] away from a communications signal source with $k = 500$, our model would predict a signal strength of $\frac{1}{10} \times 500 = 50$. For each test demonstrated in this section, the value of the scaling factor and the threshold $\mathrm{C_{THRESH}}$ are specified.

We first present a scenario with five robotic agents and a base station (the root node) in an indoor environment. The results of this test are shown in Figure 10. For this test, $k = 500$ and $\mathrm{C_{THRESH}} = 20$. Figure 10a shows both the starting configuration of the agents in the communications graph alongside the $\mathrm{COMM}(\cdot)$ values for each node with its parent. In this scenario, as "RC1", "RC2" and "RC5" have already peeled-off, the agents are included in the list of central nodes. To test the network repair behavior, we simulate

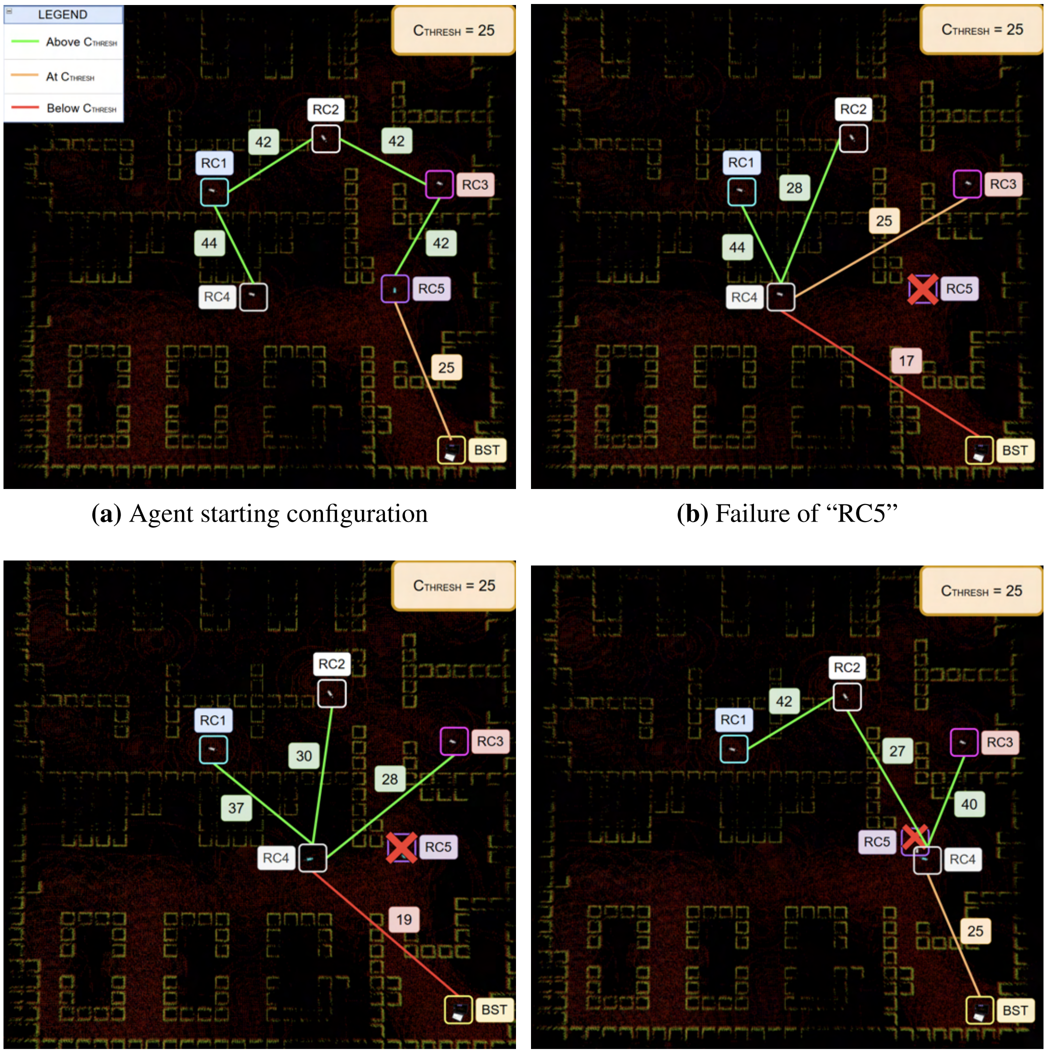

(a) Agent starting configuration

(b) Failure of “RC5”

(c) Agent “RC4” moves to its closest central node (“RC5”)

(d) Agent “RC4” repairs the network

Figure 11: The second simulation study demonstrates how the network repairing process only is initiated by agents affected by the communication dropout (“RC4”).

a failure in “RC1” causing the agent to lose connectivity with all other agents and the base station. As seen in Fig. 10b, this sudden failure of “RC1” causes the CMET$(\cdot)$ value of “RC2” to drop below C_{THRESH}. Given the logic of Algorithm 2, the network repair behavior is activated in Agent “RC2”, compelling “RC2” to move towards the next closest central node (in this case, “RC1”). As seen in Fig. 10d, “RC2” takes the place of the failed “RC1” agent, effectively repairing the network. However, as agent “RC2” moves, the CMET$(\cdot)$ value of “RC3” decreases below C_{THRESH}, as seen in Fig. 10c. This, in turn, triggers the network repair behavior in “RC3”, causing “RC3” to take the previous position of “RC2”. While this experiment contains only five agents, it demonstrates the expected cascading effect associated with the network repair behavior on all agents influenced by the failure of a central node.

The second simulation study is shown in Fig. 11. For this test, $k = 1000$

and $C_{\text{THRESH}} = 25$. As in the previous simulation experiment, Fig. 11a shows the initial configuration of the communications graph along with the $\text{COMM}(\cdot)$ values for each node with its parent. In this study, only “RC5” acts as the only non-root central node (i.e., excluding the base station) in the network, as it is the only robot that peeled-off while attaining this initial configuration. As such, we simulate a failure in agent “RC5” to investigate the reaction of the system. Figure 11b demonstrates the effect of the failure of “RC5”. The failure of “RC5” triggers the network repair behavior in “RC4”. causing it to take the place of “RC5” and repair the network (Fig. 11c). Note that none of the other robots were affected by the failure of “RC5” as “RC4” moved to repair the network, enabling the other agents to continue their tasks. This experiment demonstrates how powerful the network repair behavior can be in scenarios where only a single critical communication node fails.

5. HARDWARE TRIALS

This section details the hardware trials conducted on a team of wheeled platforms. We demonstrate both our network construction technique and network topology repair behavior on the small robotic team and conclude the section with a discussion on computation time.

5.1. Convoy & Network Repair Trials

We choose to demonstrate both the network construction behavior and the network repair behavior on a three-agent robotic team. Fig. 12 shows the time lapse of a mission in a city environment using the hardware described in Section 3.1. For this hardware trial, $k = 500$ and $C_{\text{THRESH}} = 20$.

In Fig. 12, each real world image is accompanied by the corresponding point cloud map –visualized in RViz– that is seen by the operator at the base station. The RViz images show how each node contributes to furthering the communications boundary, enabling the team to reach objectives not initially within reach of the communications system. The subfigures also demonstrate the progression of the network construction through the mission as agents change their behavior to act as communications nodes to ensure communication with the base station rather than continuing towards the objective.

Figure 12a shows the agents starting as a convoy (formation) in the vicinity of the base station. The agents are tasked with achieving the waypoints marked by the pink stars in Fig. 12. The behaviors and formation structure associated with the agent convoy are further detailed in our previous work [19,20]. As the mission progresses, “RC1” “peels-off” as it reaches the communications boundary created by the base station and establishes itself as a central node (Fig. 12b). This enables “RC2” and “RC3” to continue on the mission, as they can now use “RC1”, which is stationary, to relay messages to the base station. “RC1” effectively “extends” the communications boundary enabling “RC2” and “RC3” to reach the first waypoint.

Agents “RC2” and “RC3” then encounter a fork in the road that requires the two agents to travel in different directions to achieve two new waypoints. The agents diverge to explore each route, as shown in Fig. 12c.

To demonstrate the network repair behavior (Algorithm 2) during active operations, we then trigger a failure in “RC1” that causes it to drop from the communications network. This is shown in Fig. 12d. The failure of “RC1” causes “RC2” and “RC3” to leave the communications boundary, as the signal strength experienced by both robots drops below C_{THRESH}. The network repair behavior causes “RC3” to replace “RC1”, enabling “RC2” to continue

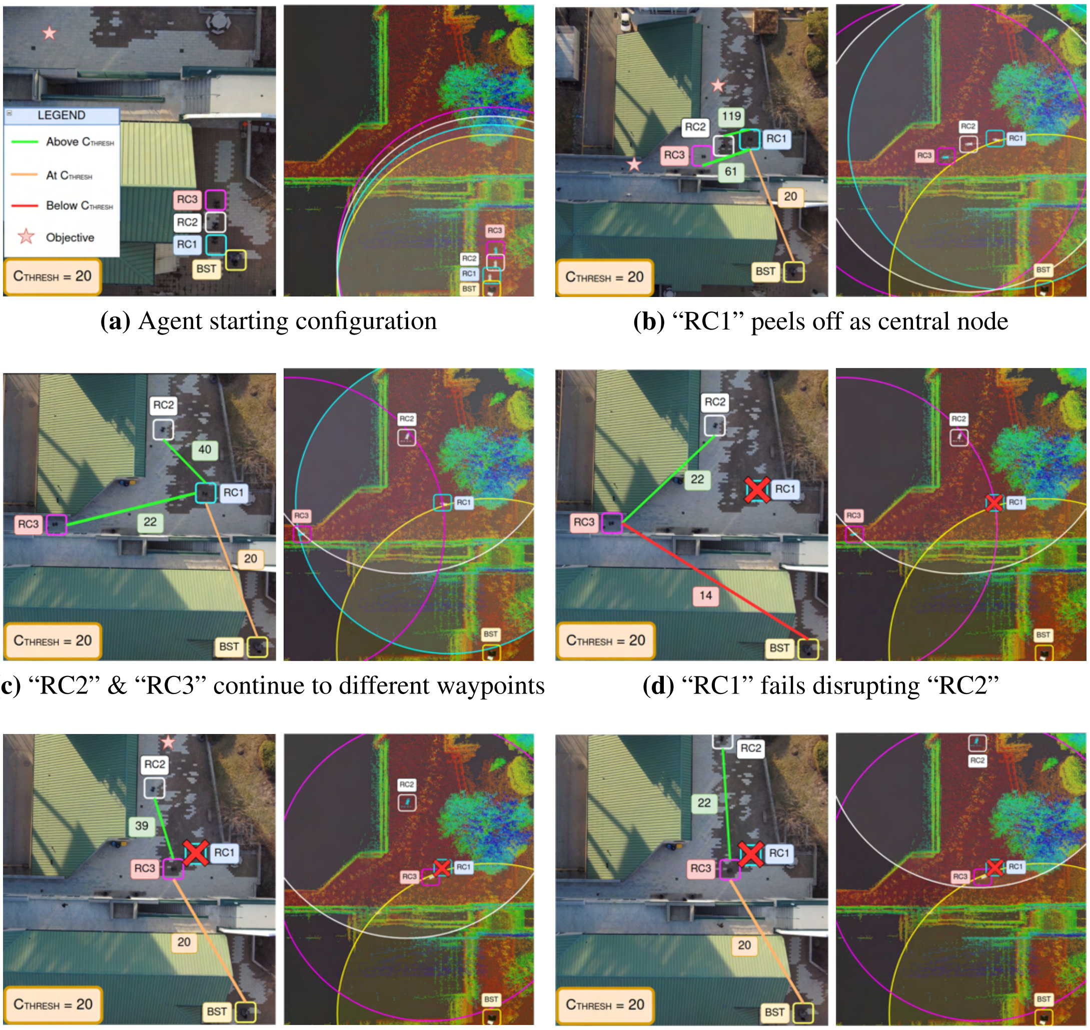

(a) Agent starting configuration

(b) “RC1” peels off as central node

(c) “RC2” & “RC3” continue to different waypoints

(d) “RC1” fails disrupting “RC2”

(e) “RC3” returns to repair the network

(f) “RC2” continues on its mission

Figure 12: A system hardware test for the network construction and network repair behaviors. Each image is composed of a full-color aerial image on the left, and a corresponding RViz visualization on the right. The RViz screen shows the base station (BST), the agents, an environmental point cloud as mapped by the agents, and the communications boundaries for each node in the communications graph.

its mission (Fig. 12e & Fig. 12f). This experiment demonstrates the functionality of both the network construction and network repair behaviors in real time on robotic hardware for a simple real-world mission.

5.2. Network Construction Trials

This section discusses the results of network construction using the “automated peel-off” behavior described in Section 3.1, and the effect of the maximin criterion for constructing the communications tree as described in Section 3.2.

Fig. 13 demonstrates the “automated peel-off” behavior in a convoy of robots, as defined in Section 3.1. For this hardware trial, we set $k = 500$ and $\mathrm{C}_{\mathrm{THRESH}} = 24$. As the $\mathrm{COMM}(\cdot)$ value of the last agent in the convoy (“RC1”) equals $\mathrm{C}_{\mathrm{THRESH}}$, it peels-off, thus acting as a stationary communication relay for the other robots in the convoy (“RC2” and “RC3”). Fig. 13a shows the convoy starting in the vicinity of the base station. Next, Fig. 13b shows the

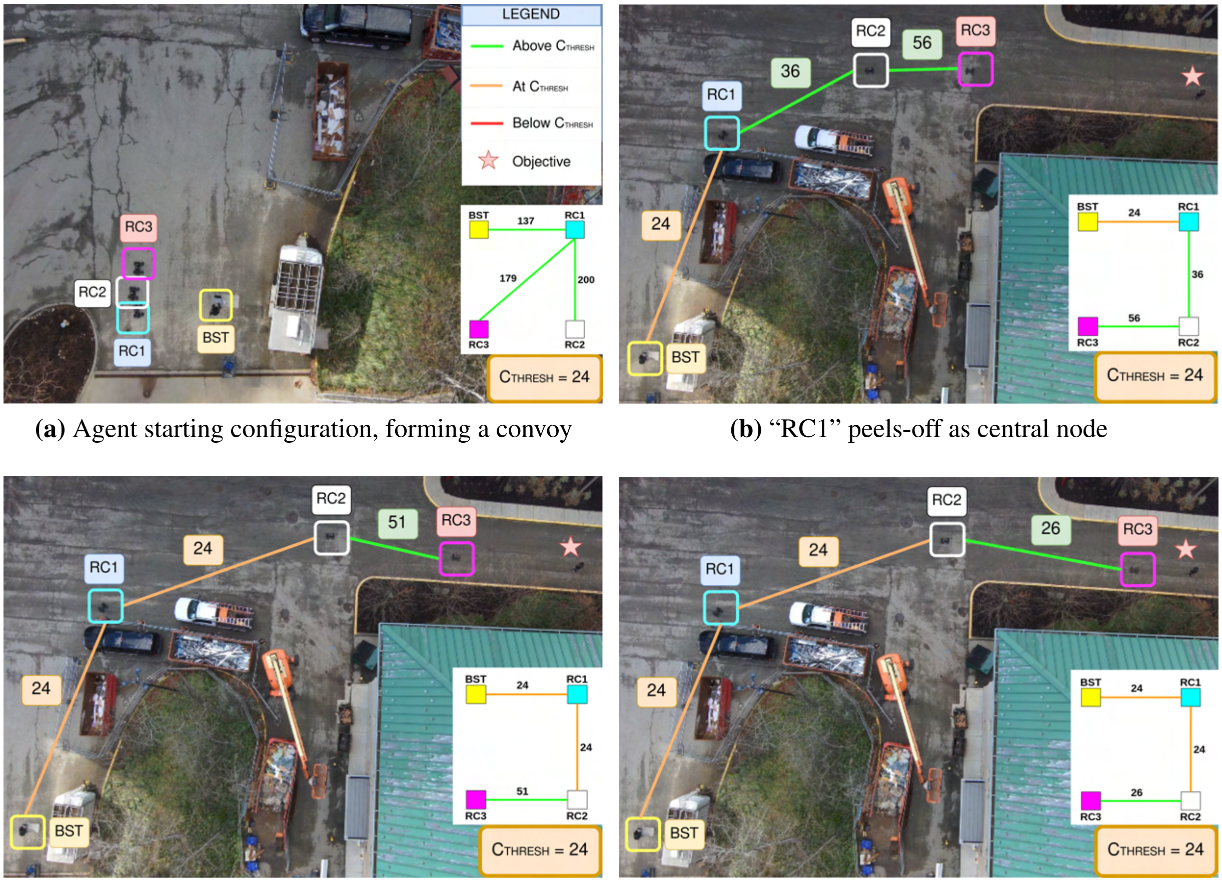

(a) Agent starting configuration, forming a convoy

(b) “RC1” peels-off as central node

(c) “RC2” peels-off as central node

(d) “RC3” reaches objective

Figure 13: Automated Peel-Off behavior, demonstrating how robots in a convoy “peel-off” and act as relays to enable mission completion. This behavior forms a crucial part of the network construction technique. Each image showcases the communication graph representing the network topology on the bottom right, and the physical layer representation of the same tree overlaid on the images.

convoy progressing towards the objective (represented as a pink star). However, “RC1” peels-off as its $\mathrm{COMM}(\cdot) = \mathrm{C}_{\mathrm{THRESH}}$. Fig. 13c shows the convoy progressing even further, by using the peeled-off “RC1” as a relay, and “RC2” peeling-off. Finally, Fig. 13d shows “RC3” reaching the objective, using “RC1” and “RC2” as communication relays. This experiment thus demonstrates the behavior of dropping communication nodes to extend the communications boundary, hence constructing the network topology.

The behavior of the maximin spanning tree is demonstrated in Fig. 14. For this hardware trial, $k = 500$ and $\mathrm{C}_{\mathrm{THRESH}} = 25$. Each image shows the $\mathrm{COMM}(\cdot)$ values between pairs of nodes and also the $\mathrm{CMET}(\cdot)$ value for each node given by the maximin tree. Fig. 14c and Fig. 14d show the two different outcomes of the experiment, with the former being when all nodes are active and the latter being when “RC4” fails.

In Fig. 14a, “RC1” connects to the base station by relaying via “RC3”. As it moves towards its objective, it finds a better connection through “RC2” as seen in Fig. 14b, and thus reaches its objective, seen in Fig. 14c. However, if “RC4”, which acts as the link between “RC2” and the base station, fails, it weakens the connection between “RC2” and the base station. This

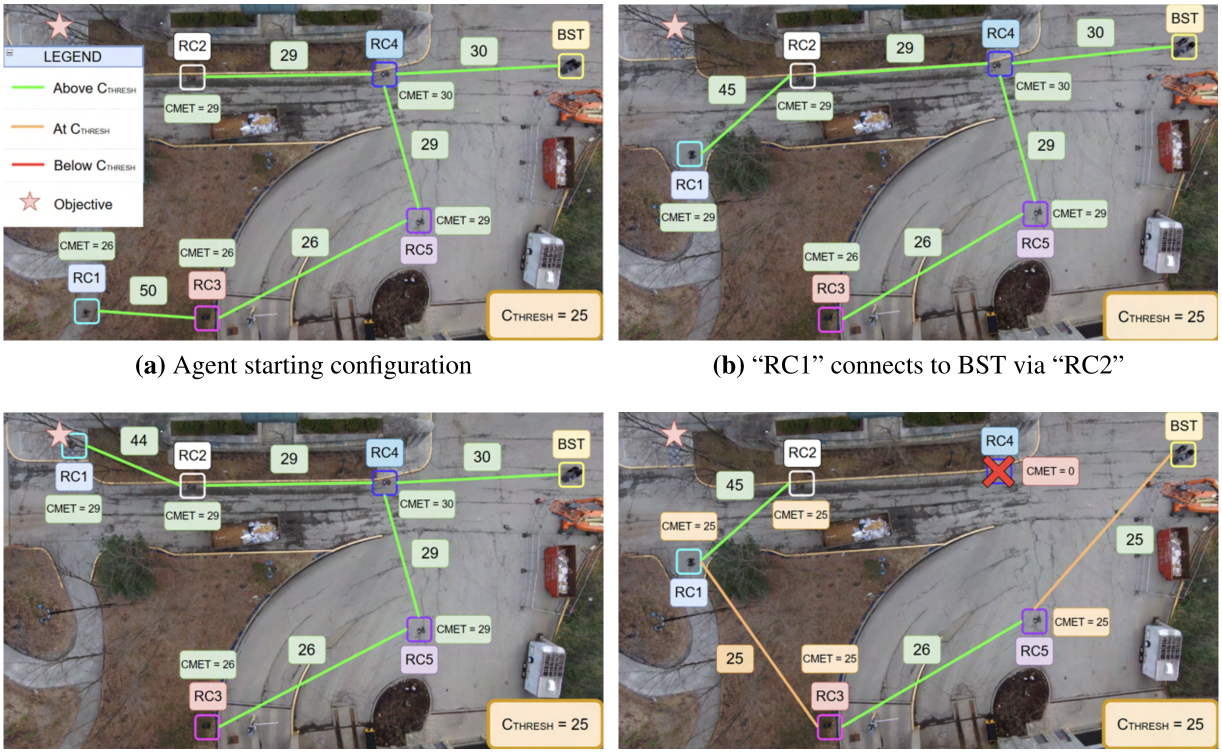

(a) Agent starting configuration

(b) "RC1" connects to BST via "RC2"

(c) "RC2" reaches objective

(d) "RC4" drops out, causing "RC1" to reach C_{THRESH} and stop

Figure 14: Demonstration of the maximin criterion for constructing the tree. This criterion considers weak links in the chain of relays (represented by the CMET$(\cdot)$ values for each node), and not just the strongest connection. Fig. 14d shows "RC1" stopping despite having a strong direct connection with "RC2". This is because the connection between "RC2" and "RC5" is weak, causing "RC2" to connect to "RC1" instead. Note that links with zero signal strength have not been shown.

causes "RC1" to connect to "RC3" instead, causing its COMM$(\cdot)$ $=$ C_{THRESH} and it to peel-off, and not reach its objective, which is evident by Fig. 14d.

The difference between the two cases is evident in Fig. 14b and Fig. 14d. In Fig. 14b the CMET$(\cdot)$ value of "RC2" is 29 whereas it is 26 for "RC3". Hence, as "RC1" aproaches "RC2", it connects via "RC2" because its CMET$(\cdot)$ value is stronger than the "RC3" CMET$(\cdot)$ value. However, in Fig. 14d the failure of "RC4" causes "RC2" to connect to "RC1" instead, as the "RC1" CMET$(\cdot)$ value is 25, which is higher than any of the other possible routes for "RC2". As a result, "RC1" remains connected to "RC3" and peels-off.

Thus, the maximin metric considers the weakest links in the network and propagates it down the chain, and all robots are assigned parents such that they have the highest possible CMET$(\cdot)$ values.

5.3. Computation Time Trials

Runtime performance is an important consideration for system operation. We demonstrate the scalability of our algorithms in a series of empirical tests, the results of which are tabulated in Fig. 15. We benchmarked the increase in computation time for the network construction algorithm as a function of network size (number of nodes). Fig. 15 reports the time taken to construct the maximin spanning tree from the communications graph. As expected, the time increases considerably as the number of nodes in the graph increases. As the network construction algorithm has been implemented in Python, significant speed gains are expected to be seen if the implementation is changed to use C++.

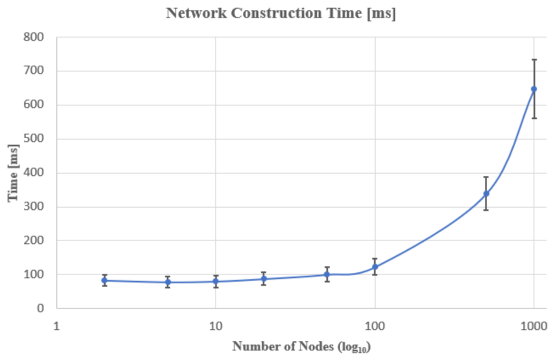

Figure 15: A summary of the computation times of the network construction algorithm. The reported times are averaged over 1000 runs, and signify the time taken by the most computationally intensive part of the algorithm i.e., the maximin spanning tree construction.

6. CONCLUSIONS

The work presented in this manuscript only scratches the surface of the many challenges in developing communications-aware robotic teaming behaviors. We have demonstrated how collaborative mobile robotic teams can be utilized to develop a mobile ad-hoc network (MANET) that enables communications in communications-deprived environments. After demonstrating the ability to form a network during a mobile robotic operation, we then demonstrate a number of recovery and repair behaviors that we have developed to address the challenges associated with real-world operations. We expect that a continued emphasis on developing communications-aware behaviors and motions will be a priority in order to support multi-agent system deployment in real-world environments. While the presented hardware demonstrations denote the technical competence of the system, multiple avenues of improvement can be made to increase the robustness and capabilities of the system.

Our experiments demonstrated that accurate communications models can be utilized to guide the creation of a communications network. Realistic models of a robot's communications systems are often highly coupled to the hardware utilized in the system. While simple geometric models are presented in this manuscript, the robotics and communications community should continue to strive to develop increasingly accurate models. Additionally, incorporating more accurate models of the communications system for the re-optimization is a priority in order to account for object interference during the formation motion.

Second, but along the same line of reasoning, a lack of an available environmental map before system operation requires the presented approach to be reactive in nature. By this, we mean that the agents must monitor the communications signal strength and then "peel-off" as a reaction to poor signal strength. Developing a system that predicts the environment map from a partial observation of the environment could be utilized to decrease the required number of agents even further by allowing the agents to predict the edge of the communications boundary before reaching it. Finally, developing an adaptive construction policy that enables the system to estimate a communications model online could provide additional benefits if environmental conditions cause the "true" communications model to be out of distribution with the deployed model.

The network repair experiments clearly indicate that a "smarter" graph optimization or search approach should be utilized to decide which agent acts to repair the network. This can result in a more effective agent utilization with minimal changes to the network topology. Furthermore, our approach relies on the A* path planner to find a feasible path back into the communications boundary. However, there can be scenarios where the planner does not find a valid path because of unobserved regions of the environment. This limitation may also be overcome by utilizing the same aforementioned map prediction algorithm.

7. REFERENCES

References

[1] DARPA, "Defense advanced research project agency, subterranean (subt) challenge (archived)," Online, 2019.

[2] M. Tranzatto, F. Mascarich, L. Bernreiter, C. Godinho, M. Camurri, S. Khattak, T. Dang, V. Reijgwart, J. Loeje, D. Wisth, S. Zimmermann, H. Nguyen, M. Fehr, L. Solanka, R. Buchanan, M. Bjelonic, N. Khedekar, M. Valceschini, F. Jenelten, M. Dharmadhikari, T. Homberger, P. D. Petris, L. Wellhausen, M. Kulkarni, T. Miki, S. Hirsch, M. Montenegro, C. Papachristos, F. Tresoldi, J. Carius, G. Valsecchi, J. Lee, K. Meyer, X. Wu, J. I. Nieto, A. Smith, M. Hutter, R. Siegwart, M. W. Mueller, M. F. Fallon, and K. Alexis, "CERBERUS: autonomous legged and aerial robotic exploration in the tunnel and urban circuits of the DARPA subterranean challenge," *CoRR*, vol. abs/2201.07067, 2022. [Online]. Available: https://arxiv.org/abs/2201.07067

[3] T. S. Vaquero, M. S. da Silva, K. Otsu, M. Kaufman, J. A. Edlund, and A.-a. Agha-mohaammadi, "Traversability-aware signal coverage planning for communication node deployment in planetary cave exploration," *International Symposium on Artificial Intelligence, Robotics and Automation in Space*, 2020.

[4] B. Morrell, K. Otsu, A. Agha, D. D. Fan, S.-K. Kim, M. F. Ginting, X. Lei, J. Edlund, S. Fakoorian, A. Bouman, F. Chavez, T. Kim, G. J. Correa, M. Saboia, A. Santamaria-Navarro, B. Lopez, B. Kim, C. Jung, M. Sobue, O. C. Peltzer, J. Ott, R. Trybula, T. Touma, M. Kaufmann, T. S. Vaquero, T. Pailevanian, M. Palieri, Y. Chang, A. Reinke, M. Anderson, F. E. T. Schöller, P. Spieler, L. M. Clark, A. Archanian, K. Chen, H. Melikyan, A. Dixit, H. Delecki, D. Pastor, B. Ridge, N. Marchal, J. Uribe, S. Dey, K. Ebadi, K. Coble, A. N. Dimopoulos, V. Thangavelu, V. S. Varadharajan, N. Palomo, A. Rosinol, A. Chatterjee, C. Kanellakis, B. Lindqvist, M. Corah, K. Strickland, R. Stonebraker, M. Milano, C. E. Denniston, S. Sahnoune, T. Claudet, S. Lee, G. Salhotra, E. Terry, R. Musuku, R. Schmid, T. Tran, A. Kourchians, J. Schachter, H. Azpurua, L. Resende, A. Kalantari, J. Nash, J. Lee, C. Patterson, J. G. Blank, K. Patath, Y. Kubo, R. Alimo, Y. Almalioglu, A. Curtis, J. Sly, T. Wells, N. T. Ho, M. Kochenderfer, G. Beltrame, G. Nikolakopoulos, D. Shim, L. Carlone, and J. Burdick, "An addendum to nebula: Toward extending team costar's solution to larger scale environments," *IEEE Transactions on Field Robotics*, vol. 1, pp. 476–526, 2024.

[5] C.-L. Lu, J.-T. Huang, C.-I. Huang, Z.-Y. Liu, C.-C. Hsu, Y.-Y. Huang, S.-C.

Huang, P.-K. Chang, Z. L. Ewe, P.-J. Huang, P.-L. Li, B.-H. Wang, L.-S. Yim, S.-W. Huang, M. R. Bai, and H.-C. Wang, "A heterogeneous unmanned ground vehicle and blimp robot team for search and rescue using data-driven autonomy and communication-aware navigation," *Field Robotics*, vol. 2, pp. 557–594, 2022.

[6] S. Scherer, V. Agrawal, G. Best, C. Cao, K. Cujic, R. Darnley, R. DeBortoli, E. Dexheimer, B. Drozd, R. Garg, I. Higgins, J. Keller, D. Kohanbash, L. Nogueira, R. Pradhan, M. Tatum, V. K. Viswanathan, S. Willits, S. Zhao, H. Zhu, D. Abad, T. Angert, G. Armstrong, R. Boirum, A. Dongare, M. Dworman, S. Hu, J. Jaekel, R. Ji, A. Lai, Y. H. Lee, A. Luong, J. Mangelson, J. Maier, J. Picard, K. Pluckter, A. Saba, M. Saroya, E. Scheide, N. Shoemaker-Trejo, J. Spisak, J. Teza, F. Yang, A. Wilson, H. Zhang, H. Choset, M. Kaess, A. Rowe, S. Singh, J. Zhang, G. A. Hollinger, and M. Travers, "Resilient and modular subterranean exploration with a team of roving and flying robots," *Field Robotics*, vol. 2, pp. 678–734, 2022.

[7] J. Gielis, A. Shankar, and A. Prorok, "A critical review of communications in multi-robot systems," *Current Robotic Reports*, vol. 3, no. 4, pp. 213–225, 2022.

[8] M. Tatum, "Cmu-ri-tr-20-19: Communications coverage in unknown underground environments," Master's thesis, Carnegie Mellon University, 2020.

[9] H. M. Ammari, "A computational geometry-based approach for planar k-coverage in wireless sensor networks," *ACM Trans. Sen. Netw.*, vol. 19, no. 2, Feb. 2023. [Online]. Available: https://doi.org/10.1145/3564272

[10] G. Kazazakis and A. Argyros, "Fast positioning of limited-visibility guards for the inspection of 2d workspaces," in *IEEE/RSJ International Conference on Intelligent Robots and Systems*, vol. 3, 2002, pp. 2843–2848.

[11] M. Ernestus, S. Friedrichs, M. Hemmer, J. Kokemuller, A. Kröller, M. Moeini, and C. Schmidt, "Algorithms for art gallery illumination," *Journal of Global Optimization*, vol. 68, 05 2017.

[12] B. Ballinger, N. Benbernou, P. Bose, M. Damian, E. D. Demaine, V. Dujmovic, R. Flatland, F. Hurtado, J. Iacono, A. Lubiw, P. Morin, V. Sacristan, D. Souvaine, and R. Uehara, "Coverage with k-transmitters in the presence of obstacles," *Journal of Combinatorial Optimization*, vol. 25, 01 2013.

[13] C. Rizzo, D. Tardioli, D. Sicignano, L. Riazuelo, J. L. Villarroel, and L. Montano, "Signal-based deployment planning for robot teams in tunnel-like fading environments," *The International Journal of Robotics Research*, vol. 32, no. 12, pp. 1381–1397, 2013.

[14] D. Tardioli, L. Riazuelo, D. Sicignano, C. Rizzo, F. Lera, J. L. Villarroel, and L. Montano, "Ground robotics in tunnels: Keys and lessons learned after 10 years of research and experiments," *Journal of Field Robotics*, vol. 36, no. 6, pp. 1074–1101, 2019. [Online]. Available: https://onlinelibrary.wiley.com/doi/abs/10.1002/rob.21871

[15] M. A. Islam, M. Maiti, Q. M. Alfred, P. K. Ghosh, and J. Sanyal, “Attenuation modelling and machine learning based snr estimation for 5g indoor link,” in *IEEE VLSI Device, Circuit and System Conference (VLSI-DCS)*, 2020.

[16] X. Wang, M. C. Gursoy, T. Erpek, and Y. E. Sagduyu, “Jamming-resilient path planning for multiple uavs via deep reinforcement learning,” in *IEEE International Conference on Communications Workshops (ICC Workshops)*, 2021.

[17] B. Woosley, P. Dasgupta, J. G. R. III, and J. Twigg, “Multi-robot information driven path planning under communication constraints,” *Autonomous Robots*, vol. 44, pp. 721–737, 2020.

[18] A. R. da Silva, L. Chaimowicz, T. C. Silva, and M. A. Hsieh, “Communication-constrained multi-robot exploration with intermittent rendezvous,” in *IEEE International Conference on Intelligent Robots and Systems (IROS)*, 2024.

[19] P. Sriganesh, J. Maier, A. Johnson, B. Shirose, R. Chandrasekar, C. Noren, J. Spisak, R. Darnley, B. Vundurthy, and M. Travers, “Modular, resilient, and scalable system design approaches - lessons learned in the years after DARPA subterranean challenge,” in *IEEE ICRA Workshop on Field Robotics*, 2024.

[20] N. Bagree, C. Noren, D. Singh, M. Travers, and B. Vundurthy, “Distributed optimal control framework for high-speed convoys: Theory and hardware results,” *IFAC-PapersOnLine*, vol. 56, no. 2, pp. 2127–2133, 2023, 22nd IFAC World Congress. [Online]. Available: https://www.sciencedirect.com/science/article/pii/S2405896323015197

[21] R. Stern, N. R. Sturtevant, A. Felner, S. Koenig, H. Ma, T. T. Walker, J. Li, D. Atzmon, L. Cohen, T. K. S. Kumar, E. Boyarski, and R. Bartak, “Multi-agent pathfinding: Definitions, variants, and benchmarks,” *Symposium on Combinatorial Search (SoCS)*, 2019.

8. CONTACT INFORMATION

Matthew Travers
Senior Systems Scientist
Carnegie Mellon University
Robotics Institute
School of Computer Science
5000 Forbes Ave.
Pittsburgh, PA
mtravers@andrew.cmu.edu

9. ACKNOWLEDGMENT

This work was in part supported by OUSD/R&E (The Under Secretary of Defense-Research and Engineering), National Defense Education Program (NDEP) / BA-1, Basic Research.

APPENDIX

This section contains a list of important notations used in this manuscript for reference.

Definition	Notation
List of assets	$\mathcal{C}$
Index set for the assets	$\mathcal{I}$
Set of agents	$\mathcal{A}$
Edges in spatial graph	E_d
Edge weights in spatial graph	w_d
Spatial graph	G_d
Operator interface node in G_d	c_0
Edges in communications graph	E_c
Edge weights in communications graph	w_c
Communications graph	G_c
Mapping from asset index to physical location	p
Signal strength between two nodes $(v_i, v_j,), v_{i,j} \in V$	w_c, COMM$(v_i, v_j,)$
Operator interface node in G_c	v_0
Minimum allowable communications edge weight	C$_{\text{THRESH}}$
Path between two nodes $(v_i, v_j,), v_{i,j} \in V$	$\pi(v_i, v_j)$
Maximin spanning tree	T
Strongest "weakest" link for (v_i, v_j) to operator node	CMET(v_i, v_j)
Set of central nodes	CN
Network topology	$\mathcal{N}$
Communications boundary	$\mathcal{B}(\mathcal{N})$
Parent node	v_p